

# Chaos-SSL: An Attention-Based Self-Supervised Learning Framework with Chaotic Transformation for Medical Image Classification

Joao Batista Florindo<sup>1</sup> <sup>a</sup>

<sup>1</sup>Institute of Mathematics, Statistics and Scientific Computing, University of Campinas, Rua Sergio Buarque de Holanda, 651, Campinas, Brazil  
florindo@unicamp.br

## Keywords:

Self-Supervised Learning, Medical Image Classification, Contrastive Learning, Chaotic Maps, Feature Fusion.

## Abstract:

Self-Supervised Learning (SSL) has emerged as a powerful paradigm to mitigate the reliance on large, annotated datasets, a common bottleneck in medical image analysis. However, standard SSL methods, which rely on simple geometric and color augmentations, may fail to capture the fine-grained, complex textural details necessary for classifying subtle pathologies. This paper introduces Chaos-SSL, a novel two-stage framework for medical image classification. In the first stage, we propose a new self-supervised pre-training strategy that leverages 1D chaotic maps (Logistic, Tent, and Sine) as a complex, non-linear augmentation for contrastive learning. We hypothesize that these chaotic transformations create “harder” and more semantically-rich views, forcing a network to learn robust representations of fine-grained medical textures. In the second stage, we introduce an attention-based fusion model that dynamically combines the specialized features from our Chaos-SSL model with the general-purpose features of a larger, ImageNet-pre-trained model. We validate our method on two public datasets: ISIC 2018 (skin lesions) and APTOS 2019 (diabetic retinopathy). Our results demonstrate that the Chaos-SSL model pre-trained with a Tent map for 30 epochs, followed by attention fusion, achieves performance fully competitive with the state-of-the-art, yielding an accuracy of 0.9261 on ISIC 2018 and 0.8726 on APTOS 2019. This significantly outperforms existing SSL methods, including several recent approaches.


## 1 INTRODUCTION

Deep learning, particularly Convolutional Neural Networks (CNNs), has become the cornerstone of modern medical image analysis, achieving human-level performance on tasks such as classification, segmentation, and detection (Huang et al., 2023). However, this success is heavily predicated on the availability of large-scale, high-quality, and expertly annotated datasets. In the medical domain, acquiring such annotations is exceptionally expensive, time-consuming, and requires specialized expertise, leading to a “data scarcity” bottleneck.

Self-Supervised Learning (SSL) has emerged as a compelling solution to this problem (Huang

et al., 2023). By designing pretext tasks that do not require human labels, SSL methods can learn rich, generalizable feature representations from vast quantities of unlabeled data. The dominant SSL paradigm, contrastive learning, (e.g., SimCLR (Chen et al., 2020) and MoCo (He et al., 2020)), trains a model to pull representations of positive pairs (e.g., two augmented views of the same image) closer together in an embedding space, while pushing negative pairs (views from different images) apart.

The efficacy of contrastive learning is fundamentally dependent on the quality of its data augmentations. Standard augmentations—such as random crops, flips, color jitter, and grayscale—are designed to be “domain-preserving” and teach invariance to simple geometric or color changes. While effective for natural images, these augmen-

<sup>a</sup>  <https://orcid.org/0000-0002-0071-0227>

tations may be insufficient for medical imaging, where pathological information is often encoded in subtle, fine-grained textural differences rather than in global object shape or color (Bisht, 2024).

This limitation has spurred research into more sophisticated SSL strategies. Some focus on pretext tasks, such as solving Jigsaw puzzles, as seen in the recent FG-SSL paper by Park & Ryu (2024), to learn spatial relationships (Park and Ryu, 2024). Others explore more complex, deformable augmentations (Arabi and Zaidi, 2024). However, a significant gap remains in developing augmentation strategies that can specifically model the complex, non-linear, and semi-chaotic nature of biological textures and disease patterns.

This paper poses a new research question: Can we create a more powerful SSL framework by replacing simple, stochastic augmentations with complex, deterministic, non-linear transformations derived from chaos theory?

We propose Chaos-SSL, a novel framework that uses 1D chaotic maps as a data augmentation strategy for contrastive learning. Our hypothesis is twofold:

1. By applying chaotic maps (Logistic, Tent, and Sine) pixel-wise to an image, we create a “hard” positive view that exhibits complex, non-linear distortions. To minimize the contrastive loss, the model is forced to learn features that are invariant to this chaotic distortion, thereby capturing essential, fine-grained textural information.
2. A single model cannot optimally capture all necessary features. Therefore, we hypothesize that a final model, which uses an “attention mechanism” to fuse the specialized, texture-aware features of our Chaos-SSL model with the robust, context-aware features of a large ImageNet-trained model, will achieve state-of-the-art performance.

To validate this, we implement a two-stage pipeline. First, we pre-train a ConvNeXt-Tiny model using our chaotic contrastive method. Second, we fuse its features with a ConvNeXt-Large model using an attention-based ensemble. We test this on the ISIC 2018 and APTOS 2019 datasets and compare our results against the state-of-the-art, including the recent FG-SSL (Park and Ryu, 2024) method. Our contributions are:

- The first (to our knowledge) application of chaotic maps as an explicit data augmentation technique for self-supervised contrastive learning.

- The design of a ChaoticTransform class compatible with standard deep learning pipelines.
- An attention-based ensemble model that effectively fuses generalist (ImageNet) features with specialist (Chaos-SSL) features.
- A comprehensive empirical study showing our method significantly outperforms prior approaches on two challenging medical classification benchmarks.

This paper is structured as follows: Section 2 reviews related work. Section 3 details our proposed methodology. Section 4 presents our experimental results. Section 5 discusses the implications of our findings, and Section 6 concludes the paper.

## 2 RELATED WORK

Our work is situated at the intersection of three active research areas: self-supervised learning in medical imaging, data augmentation, and feature fusion.

### 2.1 Self-Supervised Learning in Medical Imaging

SSL has been a major focus of the medical imaging community since 2020 (Huang et al., 2023). It is a promising solution for the challenges of small and imbalanced datasets, which are common in medicine (Espis et al., 2025). The field has evolved from early pretext tasks (e.g., rotation prediction) to more sophisticated contrastive and non-contrastive methods.

Recent works have focused on adapting SSL to the specific properties of medical data. For instance, FG-SSL (Park and Ryu, 2024) adapts the Jigsaw puzzle pretext task to medical images. It uses a “progressive Jigsaw puzzle” strategy, arguing that learning to piece together patches of different granularities helps the model learn fine-grained features. Their method, combined with BarlowTwins (a non-negative contrastive loss) (Zbontar et al., 2021), demonstrates strong performance. Other recent approaches include leveraging self-distillation (e.g., DINOv2) (Hussien et al., 2025) and combining contrastive learning with masked autoencoders (Wolf et al., 2023). These works confirm that the type of pretext task or learning signal is a critical design choice.

## 2.2 Chaos-Based Data Augmentation

While the SSL framework is important, the data augmentation pipeline is arguably one of its most critical components. Recent research, such as a 2024 study on segmentation (Arabi and Zaidi, 2024), has shown that specialized, deformable data augmentations can outperform standard contrastive learning. This suggests that creating more “difficult” or “semantically relevant” transformations is key.

Our work draws inspiration from the intersection of chaos theory and deep learning. Chaos theory provides a mathematical foundation for modeling complex, non-linear, and deterministic systems. Recent studies, such as “Neurochaos Learning” (2025) (Henry and Nagaraj, 2025), have begun to use chaotic maps (e.g., Logistic, Sine, Tent) directly within the learning paradigm, harnessing their complex dynamics. Others have explored using chaotic maps for federated learning encryption (Arévalo and Salmeron, 2023). However, the application of chaotic maps as a data augmentation technique for contrastive visual learning remains a novel and unexplored area. Our work fills this gap.

## 2.3 Attention-Based Feature Fusion

It is well-established that features from models pre-trained on different tasks (e.g., general-purpose ImageNet vs. domain-specific SSL) are often complementary. The challenge lies in how to combine them. Simple concatenation or averaging of logits is often suboptimal.

Recent literature (2023-2025) strongly advocates for more sophisticated fusion techniques. A 2023 review of medical image fusion highlights the trend toward deep learning-based methods (Zhou et al., 2023). A 2025 study proposed a “Multi-Stage Feature Fusion Network” (MSFF) that uses “Context Modulated Attention” to fuse local and global features for medical image classification (Zhang et al., 2025). Another 2025 paper introduced an “Ensemble Fusion AI” (EFAI) that intelligently concatenates features from multiple models (Shirae et al., 2025). This trend confirms our hypothesis that a learnable, attention-based fusion mechanism is a state-of-the-art approach for combining feature streams from our two distinct backbone models.

## 3 METHODOLOGY

Our proposed framework, Chaos-SSL, consists of a multi-stage pipeline designed to generate and fuse specialized feature representations. This section details the components.

### 3.1 Stage 1: Chaotic-Contrastive Pre-training (Chaos-SSL)

The first stage pre-trains a ConvNeXt-Tiny encoder using a novel self-supervised contrastive task. The core of this task is a new augmentation, the ChaoticTransform.

#### 3.1.1 The ChaoticTransform

We designed a custom torchvision transform,  $T_{chaos}$ , that applies a 1D chaotic map  $f(x)$  pixel-wise for a number of iterations  $k$ , where  $k \sim \mathcal{U}[k_{min}, k_{max}]$ . The input image tensor  $I$ , assumed to be normalized  $I \in [0, 1]^{C \times H \times W}$ , is treated as the initial state  $I^{(0)}$ . To ensure numerical stability, we clamp the input:  $I^{(0)} \leftarrow \text{clamp}(I, \epsilon, 1 - \epsilon)$ . The map is then iterated:

$$I^{(n+1)} = f(I^{(n)}) \quad \text{for } n = 0, \dots, k-1$$

The final transformed image is  $I_{chaos} = I^{(k)}$ .

We implement three distinct chaotic maps:

1. Logistic Map:  $f(x) = r \cdot x(1-x)$ , with  $r = 3.99$ .
2. Tent Map:  $f(x) = \mu \cdot \min(x, 1-x)$ , with  $\mu = 2.0$ .
3. Sine Map:  $f(x) = r \cdot \sin(\pi \cdot x)$ , with  $r = 1.0$ .

In our experiments,  $k$  is randomly sampled from  $\mathcal{U}[1, 5]$ .

#### 3.1.2 SSL Framework

We adopt a SimCLR-style contrastive framework. For each image  $I$  in a batch, we generate two views:

- View 1 ( $v_1$ ):  $v_1 = T_{std}(I)$ , where  $T_{std}$  is a composition of standard augmentations (RandomHorizontalFlip, ColorJitter, RandomGrayscale, GaussianBlur).
- View 2 ( $v_{chaos}$ ):  $v_{chaos} = T_{chaos}(T_{std}(I))$ . The chaotic map is applied after the standard augmentations.

These views are fed into our Contrastive-Model,  $M_{ssl}$ , which consists of an encoder  $E(\cdot)$  (a ConvNeXt-Tiny backbone) and a projector  $P(\cdot)$  (a 3-layer MLP):

$$z_1 = P(E(v_1)) \quad \text{and} \quad z_{chaos} = P(E(v_{chaos}))$$

The projections  $z \in \mathbb{R}^{128}$  are used to compute the NT-Xent loss. For a positive pair  $(z_i, z_j)$  from a mini-batch of size  $N$  (resulting in  $2N$  total vectors), the loss for vector  $z_i$  is:

$$\mathcal{L}_i = -\log \frac{\exp(\text{sim}(z_i, z_j)/\tau)}{\sum_{k=1, k \neq i}^{2N} \exp(\text{sim}(z_i, z_k)/\tau)}$$

where  $\text{sim}(u, v) = \frac{u^T v}{\|u\| \|v\|}$  is the cosine similarity and  $\tau$  is the temperature parameter. The total loss for the batch is  $\mathcal{L}_{NTX} = \frac{1}{2N} \sum_{i=1}^{2N} \mathcal{L}_i$ .

### 3.1.3 Training Details

We use the AdamW optimizer, with different learning rates  $LR_E$  for the encoder and  $LR_P$  for the projector. Let  $\Theta_E$  be the parameters of the encoder  $E$  and  $\Theta_P$  be the parameters of the projector  $P$ . The optimizer manages two parameter groups:

- Group 1:  $\Theta_E$ , with  $LR_E = 10^{-7}$
- Group 2:  $\Theta_P$ , with  $LR_P = 10^{-3}$

The models are trained for 15 or 30 epochs. After training,  $P$  is discarded and the weights  $\Theta_E$  are saved. Figure 1 illustrates the overall pre-training process.

## 3.2 Stage 2: Supervised Fine-Tuning of Base Models

Before fusion, we fine-tune two base models on the target task using the standard cross-entropy loss:

$$\mathcal{L}_{CE} = -\sum_{c=1}^M y_c \log(p_c)$$

where  $M$  is the number of classes,  $y_c$  is the one-hot encoded ground truth, and  $p_c$  is the predicted probability from the softmax function:  $p_c = \frac{\exp(l_c)}{\sum_{j=1}^M \exp(l_j)}$  for logits  $l$ .

- Model 1 (ImageNet-Large): A ConvNeXt-Large model, pre-trained on ImageNet, is fine-tuned for 20 epochs. It uses a CosineAnnealingLR scheduler, where the learning rate  $\eta_t$  at epoch  $t$  is:

$$\eta_t = \eta_{min} + \frac{1}{2}(\eta_{max} - \eta_{min}) \left( 1 + \cos\left(\frac{T_{cur}}{T_{max}}\pi\right) \right)$$

where  $T_{cur}$  is the current epoch and  $T_{max}$  is the total number of epochs.

- Model 2 (Chaos-SSL-Tiny): The ConvNeXt-Tiny encoder  $E$  with weights  $\Theta_E$  from Stage 1 is loaded, a new linear classifier head  $C(\cdot)$  is attached ( $M_{tiny} = C(E(\cdot))$ ), and the entire model is fine-tuned for 10 epochs.

## 3.3 Stage 3: Attention-Based Feature Fusion

The final stage combines the backbones of the two fine-tuned models,  $B_1$  (Large) and  $B_2$  (Tiny), using an attention-based feature fusion model.

### 3.3.1 Fusion Architecture

For an input  $x$ , we extract and concatenate features:

$$f_1 = B_1(x) \in \mathbb{R}^{d_1} \quad f_2 = B_2(x) \in \mathbb{R}^{d_2}$$

$$f_{concat} = [f_1, f_2] \in \mathbb{R}^{d_1+d_2}$$

A Squeeze-and-Excite attention mechanism computes an importance vector  $w_{attn}$ :

$$w_{attn} = \sigma(W_2 \cdot \delta(W_1 \cdot f_{concat}))$$

where  $W_1 \in \mathbb{R}^{d_r \times (d_1+d_2)}$  and  $W_2 \in \mathbb{R}^{(d_1+d_2) \times d_r}$  are weights of linear layers,  $d_r$  is the reduced dimension,  $\delta$  is the ReLU function, and  $\sigma$  is the Sigmoid function. The features are re-weighted using the Hadamard product  $\odot$ :

$$f_{attended} = f_{concat} \odot w_{attn}$$

A final classifier  $C_{final}$  produces the logits:

$$l_{final} = C_{final}(f_{attended}) = W_{class} \cdot f_{attended} + b_{class}$$

### 3.3.2 Fusion Training

This new model is trained with differential learning rates using AdamW. Let  $\Theta_{B1}, \Theta_{B2}$  be the backbone parameters and  $\Theta_{Head} = \{W_1, W_2, W_{class}, b_{class}\}$  be the new parameters. The optimizer manages:

- Group 1:  $\{\Theta_{B1}, \Theta_{B2}\}$ , with  $LR_{Backbone} = 10^{-6}$
- Group 2:  $\Theta_{Head}$ , with  $LR_{Head} = 10^{-4}$

The fusion model is trained for 10 epochs. Figure 2 shows the high-level diagram of the steps involved in the proposed methodology.

## 3.4 Datasets and Implementation

We evaluate our method on two publicly available medical imaging datasets.

- ISIC 2018 (Codella et al., 2018): A dataset of 10,015 dermoscopic images of skin lesions, classified into 7 categories.
- APTOS 2019 (Karthik and Dane, 2019): A dataset of 3,662 fundus images for diabetic retinopathy classification, with 5 severity grades.

All models were trained on an NVIDIA GPU (RTX 5080) using PyTorch, timm (for models), and ‘lightly’ (for NT-Xent loss) libraries.

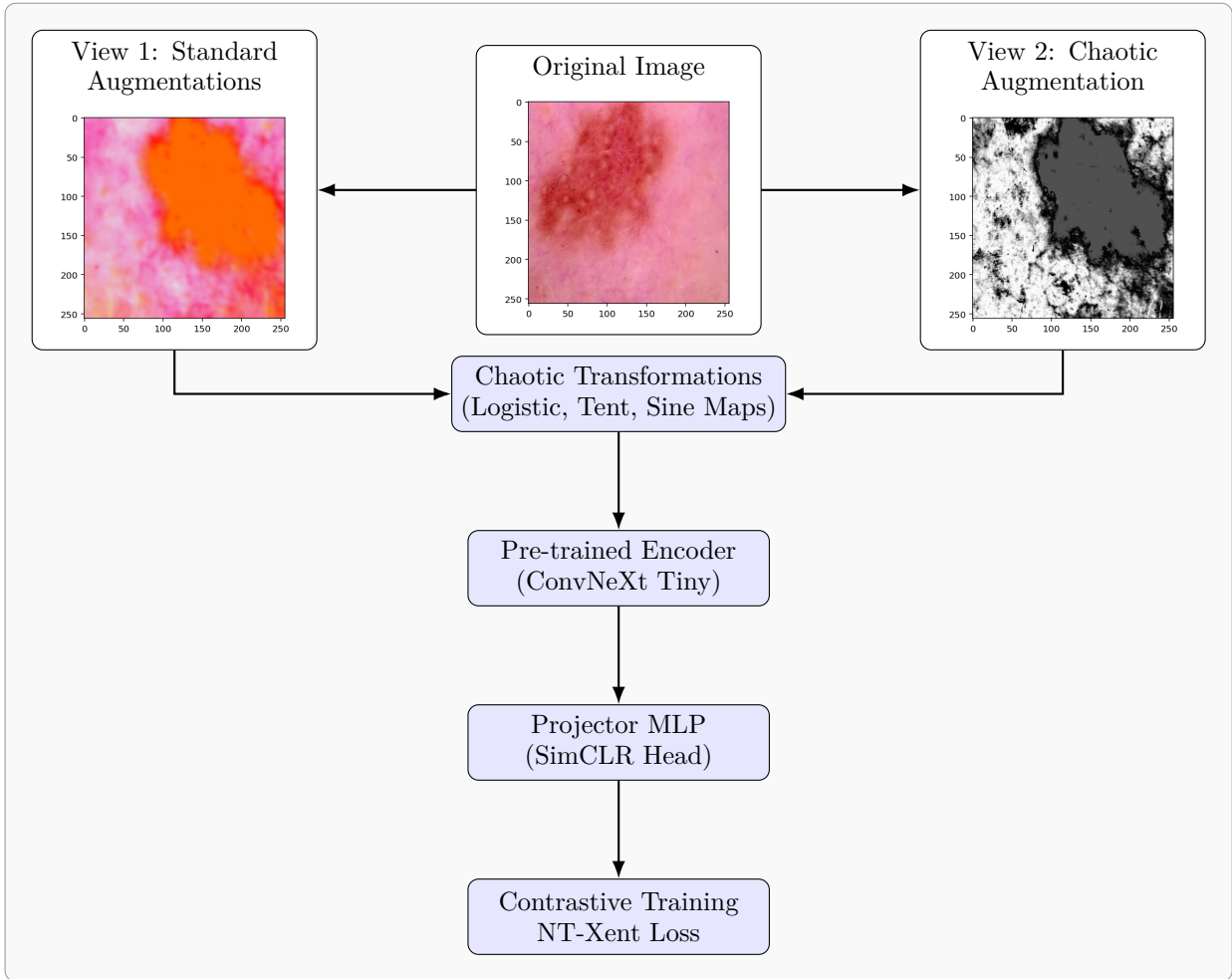


Figure 1: SSL Pre-training stage. An original image is split into two views: View 1 (Standard Augmentations) and View 2 (Chaotic Augmentation). Both views are fed into an encoder and a projector MLP, then trained using NT-Xent contrastive loss.

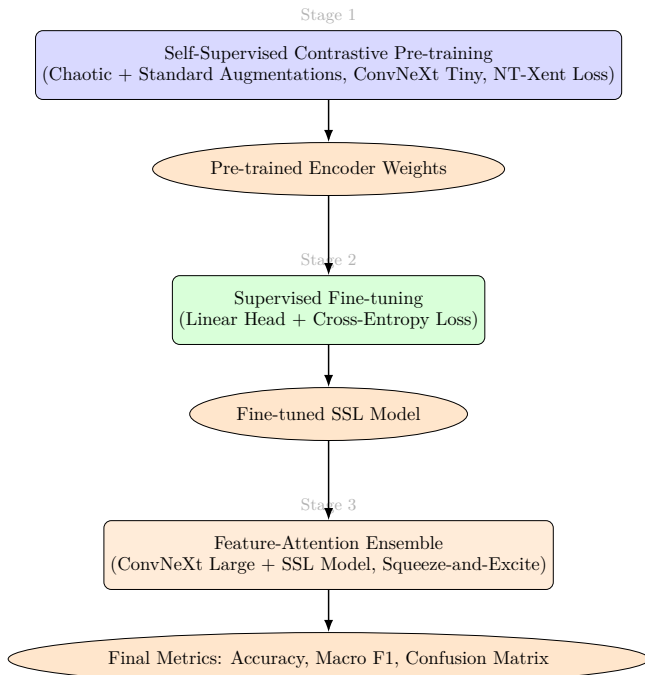


Figure 2: Overall architecture of the proposed three-stage methodology, starting with self-supervised contrastive pre-training, followed by supervised fine-tuning, and ending with a feature-attention fusion model that produces the final outcomes.

## 4 EXPERIMENTAL RESULTS

We now present the quantitative results of our Chaos-SSL framework, based on the outputs from our experimental framework. We analyze the impact of different chaotic maps and SSL training durations, and then compare our model against the state-of-the-art.

### 4.1 Performance on APTOS 2019

Table 1 shows the fusion model performance on the APTOS 2019 dataset. We observe some trends:

- **Effect of Epochs:** Increasing the SSL pre-training from 15 to 30 epochs improves performance in most cases. For the Tent map, this yields a significant jump in F1-score from 0.7323 to 0.7601.
- **Effect of Map Type:** The choice of chaotic map also has some impact. The Tent map outperforms the Logistic and Sine maps at 30 epochs, achieving the highest accuracy (0.8726) and F1-score (0.7601). At 15 epochs, Sine map is slightly superior.

Table 1: Ensemble Performance on APTOS 2019 Dataset

SSL Epochs	Chaotic Map	Accuracy	F1-Score (Macro)
15	Logistic	0.8644	0.7449
15	Sine	0.8681	0.7505
15	Tent	0.8599	0.7323
30	Logistic	0.8672	0.7484
30	Sine	0.8681	0.7483
30	Tent	0.8726	0.7601

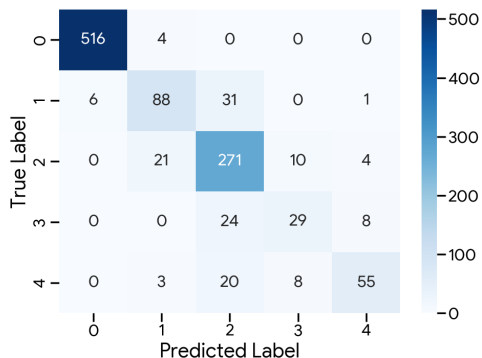


Figure 3: Confusion matrix for the best-performing model on the APTOS 2019 dataset (F1-Score: 0.7601). This corresponds to the 30-epoch Tent map SSL pre-training [cite: 394].

### 4.2 Performance on ISIC 2018

The results on the more complex, 7-class ISIC 2018 dataset (Table 2) reinforce our findings.

- **Effect of Epochs:** Again, 30 SSL epochs generally leads to better results than 15.
- **Effect of Map Type:** The Tent map once again proves to be the most effective, achieving the highest accuracy (0.9261) and F1-score (0.8706) when trained for 30 epochs. And, again, the Sine map is the best at 15 epochs.

Table 2: Ensemble Performance on ISIC 2018 Dataset

SSL Epochs	Chaotic Map	Accuracy	F1-Score (Macro)
15	Logistic	0.9198	0.8488
15	Sine	0.9245	0.8644
15	Tent	0.9195	0.8593
30	Logistic	0.9245	0.8641
30	Sine	0.9221	0.8545
30	Tent	0.9261	0.8706

### 4.3 Comparison with the Literature

The primary goal of our method is to advance the state-of-the-art in medical SSL. We compare proposed model, in its configuration with 30 epochs and Tent map, against the results reported in (Park and Ryu, 2024), which uses the same datasets.

As shown in Table 3, our Chaos-SSL framework outperforms all compared methods.

- On APTOS 2019, our 0.8726 accuracy surpasses FG-SSL’s 0.858 by 1.7% and their F1-score is surpassed by 5.6% points (0.7601 vs 0.720).
- On ISIC 2018, the gap is even larger. Our 0.9261 accuracy is 3.2% higher than FG-SSL’s 0.897, and our 0.8706 F1-score is 6.7% higher than their 0.816.

This improvement validates our hypothesis that chaotic map augmentation combined with attention fusion is a superior strategy for these fine-grained medical classification tasks.

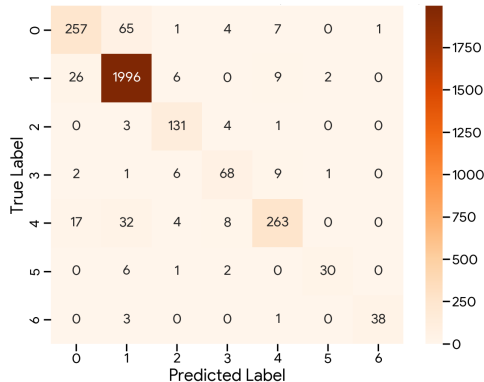


Figure 4: Confusion matrix for the best-performing model on the ISIC 2018 dataset (F1-Score: 0.8706). This corresponds to the 30-epoch Tent map SSL pre-training.

## 5 DISCUSSION

The results presented in Section IV suggest that our proposed Chaos-SSL framework is effective. We now discuss why it works, its limitations, and directions for future research.

### 5.1 Why Does Chaotic Augmentation Work?

Standard augmentations (e.g., flip, jitter) teach invariance to changes in an image that do not alter its semantic content. Our ChaoticTransform is fundamentally different. It is a non-linear, deterministic, and complex textural distortion. By creating a contrastive pair between a standard view ( $v_1$ ) and a chaotic view ( $v_{chaos}$ ), we are posing a much “harder” problem for the network: “Find the core, invariant features of this pathology, even when its fine-grained texture is warped by a complex chaotic function.”

This forces the ConvNeXt-Tiny (Model 2) to become a specialist in “textural and topological invariance.” It must learn to ignore spurious, high-frequency noise introduced by the map and focus on the underlying, persistent structure of the pathology. This is in contrast to most contrastive approaches, which focuses on learning “spatial relationships” in the pretext task. Our results suggest that for fine-grained medical images, learning textural invariance (Chaos-SSL) is a more powerful and effective pre-training signal than learning spatial arrangement.

The “Tent map’s” superior performance is intriguing. As a piecewise-linear map, its distortions may be more structured and “edge-like” compared to the smoother Sine map or the more aggressive Logistic map, making it an ideal “hard” augmentation that doesn’t completely destroy the underlying information.

### 5.2 The Power of Attention-Based Fusion

Our results are not just from the Chaos-SSL model alone; they are from the fusion ensemble. The ConvNeXt-Large (Model 1) provides a powerful, robust understanding of global shape, form, and context, learned from 1.2 million natural images. The ConvNeXt-Tiny (Model 2) provides a highly specialized, fine-grained understanding of medical textures. The feature fusion model acts as a learned “arbitrator.” Its attention mechanism dynamically learns to weigh these two feature streams, likely focusing on Model 1’s features for global context (e.g., “is this a skin lesion or an artifact?”) and Model 2’s features for fine-grained classification (e.g., “is this melanoma or a benign nevus?”).

Table 3: Comparison with literature results (as reported in (Park and Ryu, 2024))

Dataset	Method	Accuracy	F1-Score
APTOS 2019	CE (Park and Ryu, 2024)	0.812	0.608
	CL (Marrakchi et al., 2021)	0.825	0.652
	ProCo (Yang et al., 2022)	0.837	0.674
	FG-SSL (Park and Ryu, 2024)	0.858	0.720
	Chaos-SSL (Ours)	0.8726	0.7601
ISIC 2018	CE (Park and Ryu, 2024)	0.850	0.716
	CL (Marrakchi et al., 2021)	0.865	0.739
	ProCo (Yang et al., 2022)	0.887	0.763
	FG-SSL (Park and Ryu, 2024)	0.897	0.816
	Chaos-SSL (Ours)	0.9261	0.8706

### 5.3 Loss Ablation Study

“Table 3” in (Park and Ryu, 2024) provides a salient comparison of loss functions. The authors compare a KL-Divergence loss against the Barlow-Twins loss, with the latter forming their final model. In Table 4, we expand this comparison to include our final model. This shows that our combined approach of a chaotic contrastive loss (NT-Xent) followed by an attention-fusion fine-tuning yields a substantial improvement over both loss function strategies on the ISIC 2018 dataset.

Table 4: Loss Function Ablation, as reported in (Park and Ryu, 2024)

Method (on ISIC 2018)	Accuracy	F1-Score
FG-SSL (w/ KL-Div.)	0.843	0.782
FG-SSL (w/ Barlow-Twins)	0.897	0.816
Chaos-SSL (Ours)	0.9261	0.8706

### 5.4 Limitations and Future Work

Despite the suggestive results, our work has limitations:

1. **Dataset Scope:** We tested on two 2D, single-modality datasets. The method’s efficacy on 3D data (CT, MRI) or other modalities (e.g., histology) is a future research direction.
2. **Computational Cost:** The final ensemble model requires running two backbones (Large and Tiny), increasing inference time. For clinical deployment, model distillation into a single, compact network would be necessary.
3. **Interpretability:** While we have a hypothesis for why the Tent map works best, it remains an empirical finding. A deeper theoretical

analysis of the interaction between chaotic map properties and learned feature invariances is needed.

Future work will proceed in three main directions:

- “Expanding Augmentations”: Exploring compositions of chaotic maps (e.g.,  $f(x) = f_{logistic}(f_{tent}(x))$ ), as suggested by recent work (Henry and Nagaraj, 2025), or applying maps in the frequency domain.
- “Expanding Frameworks”: Applying Chaotic-Transform to other SSL frameworks, such as Masked Autoencoders (MAE) or self-distillation (DINO).
- “Expanding Domains”: Validating this approach on 3D medical tasks and in other data-scarce, fine-grained domains (e.g., satellite imagery, materials science).

## 6 CONCLUSION

This paper addressed the critical challenge of learning fine-grained representations in data-scarce medical imaging. We introduced Chaos-SSL, a novel self-supervised framework that moves beyond simple geometric augmentations. By using chaotic maps as a complex, non-linear transformation for contrastive learning, we successfully pre-trained an encoder to be invariant to high-frequency textural distortions.

We further proposed an attention-based fusion model that effectively combines the specialized, fine-grained features from our Chaos-SSL model with the robust, general-purpose features of a large ImageNet model.

Our comprehensive experiments on the ISIC 2018 and APTOS 2019 datasets showed that our

method, using a 30-epoch Tent map pre-training, achieves results competitive with the state-of-the-art. It significantly outperforms prior SSL methods, including the recent FG-SSL approach, on both accuracy and F1-score. This work validates the use of chaotic dynamics as a powerful new tool in the self-supervised learning-based data augmentation, opening new avenues for developing highly specialized models for complex medical image analysis.

## ACKNOWLEDGEMENTS

During the preparation of this work the authors used Google Gemini in order to improve readability and language. After using this tool, the authors reviewed and edited the content as needed and take full responsibility for the content of the publication.

## REFERENCES

- Arabi, H. and Zaidi, H. (2024). Contrastive learning vs. self-learning vs. deformable data augmentation in semantic segmentation of medical images. *Journal of Imaging Informatics in Medicine*, 37(6):3217–3230.
- Arévalo, I. and Salmeron, J. L. (2023). A chaotic maps-based privacy-preserving distributed deep learning for incomplete and non-iid datasets.
- Bisht, Y. S. (2024). Enhancing medical image classification using self-supervised transfer learning. In *3rd Int. Conf. for Innovation*.
- Chen, T., Kornblith, S., Norouzi, M., and Hinton, G. (2020). A simple framework for contrastive learning of visual representations. In *Proc. ICML*.
- Codella, N. C., Gutman, D., Celebi, M. E., Helba, B., Marchetti, M. A., Dusza, S. W., Kalloo, A., Liopyris, K., Mishra, N., Kittler, H., et al. (2018). Skin lesion analysis toward melanoma detection: A challenge at the 2017 international symposium on biomedical imaging (isbi), hosted by the international skin imaging collaboration (isic). In *Proc. ISBI*.
- Espis, A., Marzi, C., and Diciotti, S. (2025). Comparative analysis of supervised and self-supervised learning with small and imbalanced medical imaging datasets. *Scientific Reports*, 15(1):32345.
- He, K., Fan, H., Wu, Y., Xie, S., and Girick, R. (2020). Momentum contrast for unsupervised visual representation learning. In *Proc. CVPR*.
- Henry, A. and Nagaraj, N. (2025). Neurochaos learning for classification using composition of chaotic maps.
- Huang, S.-C., Pareek, A., Jensen, M., Lungren, M. P., Yeung, S., and Chaudhari, A. S. (2023). Self-supervised learning for medical image classification: a systematic review and implementation guidelines. *npj Digital Medicine*, 6(74).
- Hussien, A., Elkhateb, A., Saeed, M., Elsabawy, N. M., Elnakeeb, A. E., and Elrashidy, N. (2025). Explainable self-supervised learning for medical image diagnosis based on dino v2 model and semantic search. *Scientific Reports*, 15(1):32174.
- Karthik, M. and Dane, S. (2019). Aptos 2019 blindness detection. *Kaggle*.
- Marrakchi, Y., Makansi, O., and Brox, T. (2021). Fighting class imbalance with contrastive learning. In *International conference on medical image computing and computer-assisted intervention*, pages 466–476. Springer.
- Park, W. and Ryu, J. (2024). Fine-grained self-supervised learning with jigsaw puzzles for medical image classification. *Computers in Biology and Medicine*, 174.
- Shirae, S., Debsarkar, S. S., Kawanaka, H., Aronow, B., and Prasath, V. S. (2025). Multimodal ensemble fusion deep learning using histopathological images and clinical data for glioma subtype classification. *IEEE Access*.
- Wolf, D., Payer, T., and et al. (2023). Self-supervised pre-training with contrastive and masked autoencoder methods for dealing with small datasets in deep learning for medical imaging. *Scientific Reports*.
- Yang, Z., Pan, J., Yang, Y., Shi, X., Zhou, H.-Y., Zhang, Z., and Bian, C. (2022). Proco: Prototype-aware contrastive learning for long-tailed medical image classification. In *International conference on medical image computing and computer-assisted intervention*, pages 173–182. Springer.
- Zbontar, J., Jing, L., Misra, I., LeCun, Y., and Deny, S. (2021). Barlow twins: Self-

supervised learning via redundancy reduction. In Proc. ICML.

Zhang, R., Luo, X., Lv, J., Cao, J., Zhu, Y., Wang, J., and Zheng, B. (2025). Enhancing medical image classification with context modulated attention and multi-scale feature fusion. IEEE Access.

Zhou, T., Cheng, Q., Lu, H., Li, Q., Zhang, X., and Qiu, S. (2023). Deep learning methods for medical image fusion: A review. Computers in Biology and Medicine, 160.